Monitoring the Crystal Growth and Interconversion of New Coordination Networks in the Self-assembly of MCl_2 Salts (M = Co, Ni, Cu, Cd) and 1,3-Bis(4-pyridyl)propane

Lucia Carlucci,[†] Gianfranco Ciani,*[,‡] Massimo Moret,[§] Davide M. Proserpio,[‡] and Silvia Rizzato[‡]

Dipartimento di Biologia Strutturale e Funzionale, Università dell'Insubria, via J. H. Dunant 3, 21100 Varese, Italy, Dipartimento di Chimica Strutturale e Stereochimica Inorganica and Centro CNR, Università degli Studi di Milano, via G. Venezian 21, 20133 Milano, Italy, and Dipartimento di Scienza dei Materiali, Università di Milano-Bicocca, via Cozzi 53, 20125 Milano, Italy

Received September 6, 2001
Revised Manuscript Received October 30, 2001

The current interest for the self-assembly of networked coordination polymers,[1] because of their potential properties as novel zeolite-like materials,[2] for molecular sieving, ion exchange, gas storage, molecular sensing, and catalysis, has afforded many noteworthy two-dimensional (2D) and three-dimensional (3D) frames. However, the crystal engineering of networks with desired topologies and specific properties still remains a hard challenge, and the variety of factors that can influence a particular self-assembly process are not yet well understood. Indeed, besides a careful choice of suitable building blocks and reaction conditions, no model for the network formation from the solution is presently available. Because the final outcome of the crystallization can be driven by the details of the process, the investigation of these factors cannot be less important than the correct selection of the reagents.

In this concern the use of microscopic techniques at different levels (optical or scanning probe microscopy, SPM), paralleling the crystallographic structural characterization of the products, can be useful for many purposes, including the following: (i) the study of the factors influencing the kinetic nucleation and crystal growth; (ii) the diagnostic monitoring of the crystallization process to reveal the possible crystal transformations with time or upon a change in the reaction conditions; (iii) the analysis of correlations between crystal structure and crystal morphology, and, particularly, the growth rates in different directions; (iv) the investigation of the surface phenomena under crystal transformation. Few studies concerning some of these features have been reported for metal complexes[3] and, in particular, none, to our knowledge, for coordination polymers.[4] Indeed, we have recently obtained interesting results from the AFM monitoring of the nanoporous behavior of a catenated spongelike 3D coordination network.[5,6]

We have therefore investigated, using the above approach, the networking ability of the conformationally flexible bidentate ligand 1,3-bis(4-pyridyl)propane (bpp) with the chlorides of M^{2+} cations (M = Co, Ni, Cu, Cd), in variated crystallization conditions. We report here on these studies, carried out at a phenomenological level, that have lead to some interesting and unpredictable results.

Different polymeric species have been obtained, depending on the solvent system. Two main bulk products have been isolated with all the metal salts by the direct reactions carried out using a bpp to MCl_2 molar ratio of 2:1, that is, the one-dimensional (1D) polymer $[M(bpp)_3Cl_2]$ from water solutions, and the interpenetrated diamondoid network $[M(bpp)_2Cl_2]$ from mixed solvent systems involving water and an organic solvent (alcohols, acetone, dichloromethane, and others).[7] We have then focused our investigation on the copper system. However, in the attempt of obtaining the 1D polymer from water, we have also observed the preliminary formation of crystals of a third species. We therefore describe here the structures of the three copper polymers, namely, $[Cu(bpp)_3Cl_2]\cdot 2H_2O$ (**1**), $[Cu(bpp)_2Cl]Cl\cdot 1.5H_2O$ (**2**), and $[Cu(bpp)_2Cl_2]\cdot 2.75H_2O$ (**3**) that are 1D, 2D, and 3D polymers, respectively.[8−10]

This system has been the object of growth studies using optical microscopy. We have observed that the formation of **1** is preceded by the nucleation and growth of crystals of **2**, not observed in the bulk reactions of the other salts. Both **1** and **2** are obtained from water solutions of the reagents, but in successive periods of time. The crystal growth and the solid transformation mediated by the solvent have been followed by means

* To whom correspondence should be addressed. Fax: +(39)0250314454. E-mail: davide@csmtbo.mi.cnr.it.
[†] Università dell'Insubria.
[‡] Università di Milano.
[§] Università di Milano-Bicocca.

(1) (a) Hoskins, B. F.; Robson, R. *J. Am. Chem. Soc.* **1990**, *112*, 1546. (b) Robson, R.; Abrahams, B. F.; Batten, S. R.; Gable, R. W.; Hoskins, B. F.; Liu, J. *Supramolecular Architecture*; American Chemical Society: Washington, DC, 1992; Chapter 19. (c) Bowes, C. L.; Ozin, G. A. *Adv. Mater.* **1996**, *8*, 13. (d) Eddaoudi, M.; Moler, D. B.; Li, H.; Chen, B.; Reineke, T. M.; O'Keeffe, M.; Yaghi, O. M. *Acc. Chem. Res.* **2001** *34*, 319. (e) Munakata, M.; Wu, L. P.; Kuroda-Sowa, T. *Adv. Inorg. Chem.* **1999** *46*, 173. (f) Hagrman, P. J.; Hagrman, D.; Zubieta, J. *Angew. Chem., Int. Ed.* **1999**, *38*, 2638. (g) Moulton, B.; Zaworotko, M. J. *Chem. Rev.* **2001**, *101*, 1629.

(2) See, for example, (a) Janiak, C. *Angew. Chem., Int. Ed. Engl.* **1997**, *36*, 1431. (b) Keppert, C. J.; Rosseinsky, M. J. *Chem. Commun.* **1998**, 31. (c) Goodgame, D. M. L.; Grachvogel, D. A.; Williams, D. J. *Angew. Chem., Int. Ed.* **1999**, *38*, 153.

(3) See, for example, (a) Waizumi, K.; Masuda, H.; Ohtaki, H.; Tsukamoto, K.; Sunagawa, I. *Bull. Chem. Soc. Jpn.* **1990**, *63*, 3426. (b) Chun, H.; Bernal, I. *Cryst. Growth Des.* **2001**, *1*, 67.

(4) The self-assembly of metallogrids to give monolayers has been investigated by combined X-ray diffraction and scanning probe microscopy: (a) Semenov, A.; Spatz, J. P.; Lehn, J.-M.; Weidl, C. H.; Schubert, U. S.; Möller, M. *Appl. Surf. Sci.* **1999**, *144−145*, 456. (b) Weissbuch, I.; Baxter, P. N. W.; Kuzmenko, I.; Cohen, H.; Cohen, S.; Kjaer, K.; Howes, P. B.; Als-Nielsen, J.; Lehn, J.-M.; Leiserowitz, L.; Lahav, M. *Chem. Eur. J.* **2000**, *6*, 725.

(5) Carlucci, L.; Ciani, G.; Moret, M.; Proserpio, D. M.; Rizzato,S. *Angew. Chem., Int. Ed.* **2000**, *39*, 1506.

(6) Similar investigations by AFM monitoring have been performed on hydrogen-bonded systems: (a) Palmore, G. T. R.; Luo, T. J.; Martin, T. L.; McBride-Wieser, M. T.; Voong, N. T.; Land, T. A.; De Yoreo, J. J. *Trans. Am. Crystallogr. Assoc.* **1998**, *33*, 45. (b) Ester, G. R.; Halfpenny, P. J. *J. Cryst. Growth* **1998**, *187*, 111.

(7) The rate of reaction and crystallization, in the same experimental conditions, is different for the M^{2+} cations, namely, Cd > Cu ≫ Co ≈ Ni, but in all cases it has been possible to obtain large and well-shaped crystals of the two species by means of different crystallization techniques or by modification of crystallization parameters.

10.1021/cm011235s CCC: $22.00
Published on Web 12/08/2001

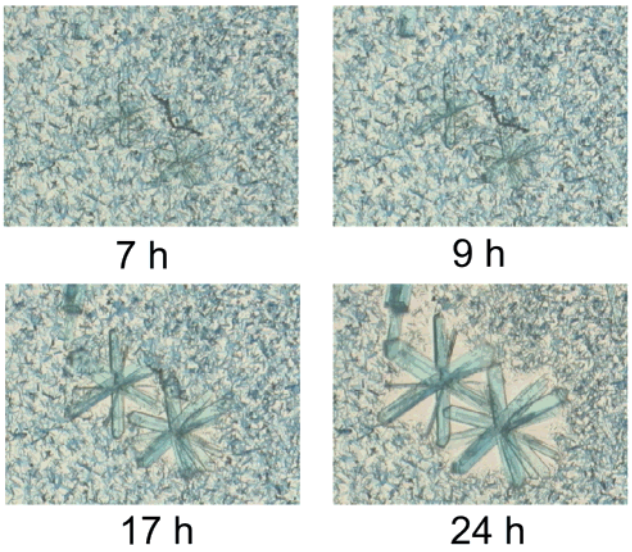

Figure 1. Monitoring of the crystal transformation **2** → **1**; small crystals on the background belong to **2**. Crystals of **1** nucleated approximately after 2 h since solution mixing (elapsed time reported; 2.5 mm on the long side).

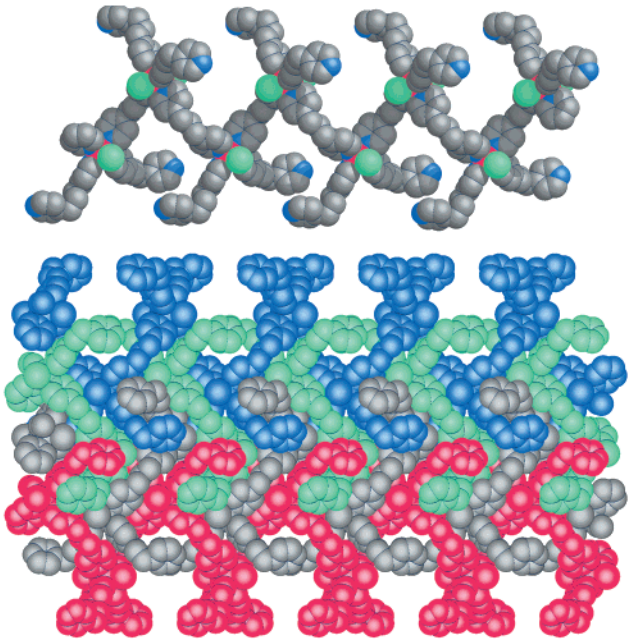

Figure 2. View of a single zigzag chain in coumpound **1** (top) and of the interdigitation of the polymers (bottom) in the (0 0 1) plane (horizontal axis **a**, vertical axis **b**). The coordination geometry is distorted octahedral and relevant bond parameters are as follows: Cu−N 2.050(4)−2.054(4) Å; Cu−Cl 2.795(1)−2.802(1) Å.

of an optical microscope coupled to a CCD camera with automatic time series image acquisition. The pictures show (Figure 1) that after a few hours a large amount of dark-blue crystals of **2** were formed as the unique product, and then the system evolved to **1**, which gives larger crystals of a lighter blue color with a characteristic morphology, while the crystals of **2** were progressively destroyed. The transformation (at room temperature) takes place with different rates at different ligand-to-metal molar ratios. Relatively high concentrations of the reagents and/or lower ligand-to-metal ratios favor the formation of crystals of **2** at the expense of **1**.[11] When the proper conditions are used, therefore, the

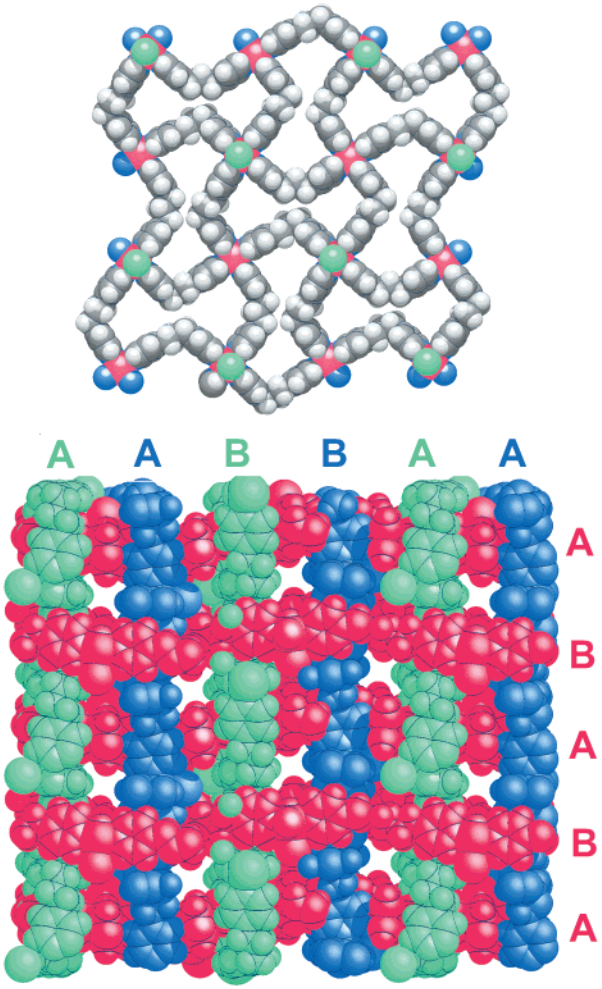

Figure 3. View of a single (4,4) layer in **2** (top) and of the 3D architecture formed by interpenetration of the three sets of layers down the **a** axis (bottom). The stacking of the layers is *ABAB* for all three sets. The open channels running down [1 0 0] are evidenced. Relevant bond parameters are as follows: Cu−N 2.015(8)−2.089(8) Å; Cu−Cl 2.499(3)−2.537(4) Å.

2 → **1** transformation can be stopped or driven to completion so that we were able to obtain pure crystal samples of both species suitable for a single-crystal X-ray analysis.[12]

The structure of compound **1** consists of zigzag Cu(bpp) chains all running in the [1 0 0] direction and exhibiting also two monocoordinated ligands *per* metal atom (Figure 2); these parallel 1D polymers (with a period equal to **a,** 17.19 Å) are arranged in (0 0 1) planes

(8) Both compounds **1** and **2** are obtained from water solution as pure samples. For **1**: a solution of the bpp ligand (24.1 mg; 0.122 mmol) in water (4 mL) is added to a stirred solution of $CuCl_2 \cdot 2H_2O$ (6.8 mg; 0.040 mmol) dissolved in 4 mL of water. A blue precipitate formed immediately, which was left to stir for 40 min, filtered, and dried under vacuum (yield: 46%). **2** is obtained following the above procedure with 23.7 mg (0.120 mmol) of bpp ligand and 10.3 mg (0.060 mmol) of $CuCl_2 \cdot 2H_2O$ (yield: 40%). The synthesis of **3** was carried out as follows: a solution of bpp (40.5 mg; 0.204 mmol) in ethanol (4 mL) was added to a stirred solution of $CuCl_2 \cdot 2H_2O$ (17.4 mg; 0.102 mmol) dissolved in 4 mL of ethanol. A blue precipitate formed immediately, which was left to stir for 40 min, filtered, and dried under vacuum (yield: 52%). The pure nature of these powdered samples was confirmed by XRPD methods. Variable elemental analyses were obtained because of the loss in the air of solvent molecules (3−4%). For example, calcd. for **1**, $C_{39}H_{46}Cl_2CuN_6O_2$, C 61.21, H 6.06, N 10.98; found, C 61.9, H 6.0, N 11.1; for **2**, $C_{26}H_{31}Cl_2CuN_4O_{1.5}$, C 55.96, H 5.60, N 10.04; found, C 56.8, H 5.5, N 10.1; for **3**, $C_{26}H_{33.5}Cl_2CuN_4O_{2.75}$, C 53.79, H 5.82, N 9.65; found, C 54.5, H 5.8, N 9.7.

with high interdigitation of their dangling ligands. The layers of interdigitated chains stack along the **c** crystallographic axis, interacting in this direction only via $\pi-\pi$ contacts involving the uncoordinated pyridyl rings.[13] Thermogravimetric analysis shows that compound **1** is stable up to ≈120 °C.

The structure of **2** consists of tassellated (4,4) sheets (Figure 3, top) based on five-coordinated copper atoms in a square-pyramidal geometry (with four equatorial pyridyl groups and an axial chloride ion). There are three almost identical but crystallographically independent sets of sheets (in red, green, and blue in Figure 3, bottom), which lie parallel to the (0 1 0) (red) and (0 0 1) (green and blue) planes and display "inclined" interpenetration,[14,15] resulting in an overall 3D array. The space-filling model of **2** down the **a** axis, illustrated in Figure 3 (bottom), clearly shows that there are open channels within the network (four per unit cell of free volume of ≈280 Å^3 each) occupied by the included water molecules and free Cl^- anions (omitted for clarity).

Despite the different stoichiometry, the **2** → **1** transformation is spontaneous also if it implies that part of the copper remains unreacted; **1** is clearly favored by an excess of bpp, but the formation of **2** is observed even at a large ligand-to-metal stoichiometric excess. The process seems entropy-favored but the mechanism is not clear.

Differently from the behavior in water solution, the presence of ethanol or other organic solvents (methanol, acetone, and CH_2Cl_2) leads to the formation of crystals of **3** only.

The structure of **3** consists of four interpenetrating diamondlike networks of octahedral metal centers linked by bpp bridges, which occupy the four equatorial positions of the copper coordination sphere, which is completed by two Cl^- anions (in the trans positions) (see Figure 4, left). The four independent frameworks are related by translation along the **c** tetragonal axis in the usual interpenetration topology for diamondoid frames.[14,15] However, in a set of adamantane cages the ligands display patterns that are rotated by 90° about **c** upon passing from one frame to the successive one (Figure 4, right). This creates isolated cavities to host the solvent molecules, in contrast to the typical open channels in the normal "parallely" interpenetrated *n*-fold diamondlike nets. Indeed, despite interpenetration, the coordination network of **3** still contains large voids, filled by solvated molecules, mainly of water.[16]

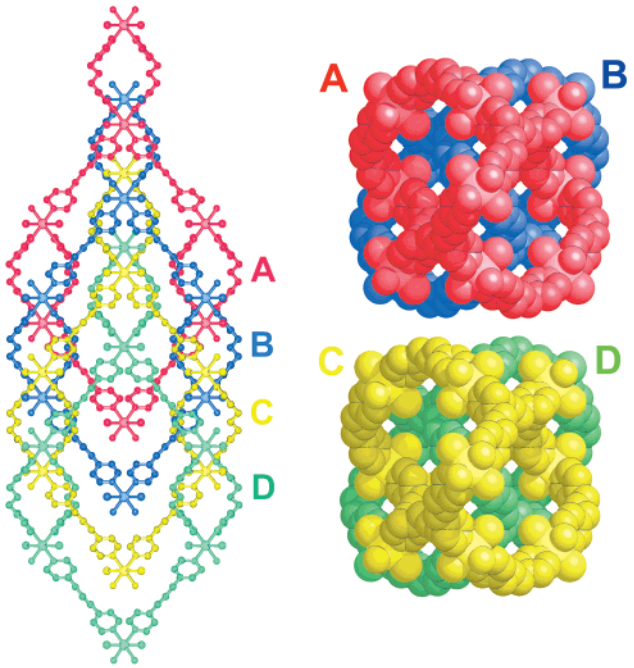

Figure 4. View of the 4-fold interpenetrated diamondoid network in compound **3** (left) and of the isolated solvent-containing chambers represented down the [0 0 1] direction. Relevant bond parameters are as follows: Cu−N 2.036(7)−2.069(5) Å; Cu−Cl 2.679(2)−2.832(3) Å.

The great influence of the solvent in this system has been confirmed by direct observation by optical microscopy of the trasformation to compound **3** of crystals of both **1** and **2** suspended in ethanol, according to the overall Scheme. Likely ethanol has a templating effect on the formation of **3**, by filling the isolated cavities.[16] All the transformations have been confirmed by XRPD methods.

A morphological analysis has also been carried out, with face indexing of all the crystalline species to correlate the crystallographic parameters, and therefore the polymerization vectors of the networks, to the growth directions of crystals.

(9) Crystal data for **1**, $C_{39}H_{46}Cl_2CuN_6O_2$: monoclinic, space group *I*2/*a* (No. 15), a = 17.191(1) Å, b = 16.242(1) Å, c = 26.859(2) Å, β = 91.59(1)°, V = 7496.4(8) Å^3, Z = 8, ρ_{calcd} = 1.356 Mg·m^{-3}, final R1 value 0.0788 for 6615 independent reflections [$I > 2\sigma(I)$]. Crystal data for **2**, $C_{26}H_{31}Cl_2CuN_4O_{1.5}$: orthorhombic, space group $P2_12_12_1$ (No. 19), a = 16.314(1) Å, b = 18.211(1) Å, c = 36.247(3) Å, V = 10768.8(14) Å^3, Z = 16, ρ_{calcd} = 1.377 Mg·m^{-3}, final R1 value 0.0824 for 15 361 independent reflections [$I > 2\sigma(I)$]. Crystal data for **3**, $C_{26}H_{33.5}Cl_2CuN_4O_{2.75}$: tetragonal, space group $I4_1/a$ (No. 88), a = 17.221(1) Å, b = 17.221(1) Å, c = 40.965(2) Å, V = 12148.7(9) Å^3, Z = 16, ρ_{calcd} = 1.270 Mg·m^{-3}, final R1 value 0.0991 for 3921 independent reflections [$I > 2\sigma(I)$]. The data collections were performed at room temperature for **1** and **2** and at 223 K for **3** on a Bruker SMART CCD area-detector diffractometer, using Mo Kα radiation (λ = 0.71073 Å) by the ω-scan method, within the limits 3° < θ < 25°. Empirical absorption corrections (SADABS) were applied. The structure was solved by direct methods (SIR97) and refined by full-matrix least-squares on F^2 (SHELX-97). Anisotropic thermal factors were assigned to all the non-hydrogen atoms but to the water molecules with half occupancy. Compound **2** shows a disorder produced by partial inversion of the square-pyramidal geometry at each copper center and modeled by two components of 84 and 16% for copper and the bounded chlorine atom. The assignment of the absolute structure for **2** was confirmed by the statistics and the refinement of the absolute structure parameter as implemented in SHELX-97 to a value of 0.00(2). All the diagrams were generated using the SCHAKAL 97 program.

(10) Different structures due to slight changes in the crystallization conditions have already been reported for copper species. See, for example, Janiak, C.; Scharmann, T. G.; Gunther, W.; Hinrichs, W.; Lentz, D. *Chem. Ber.* **1996**, *129*, 991. Janiak, C.; Uehlin, L.; Wu, H. P.; Klufers, P.; Piotrowski, H.; Scharmann, T. G. *J. Chem. Soc., Dalton Trans.* **1999**, 3121.

(11) Preliminary studies on the influence of the temperature show that the formation of **2** seems favored by an increase of *T*.

(12) The transformations described here can be related by analogy to the kinetic and thermodynamic factors recently reviewed by Bernstein et al. for concomitant polymorphs: Bernstein, J.; Davey, R. J.; Henck, J.-O. *Angew. Chem., Int. Ed.* **1999**, *38*, 3441.

(13) Janiak, C. *J. Chem. Soc., Dalton Trans.* **2000**, 3885.

(14) Batten, S. R.; Robson, R. *Angew. Chem., Int. Ed.* **1998**, *37*, 1461.

(15) Batten, S. R. *CrystEngComm* **2001**, 18.

(16) An analysis of these regions in a unit cell, performed by neglecting all the solvent molecules, shows four equivalent isolated chambers, probably templated by the ethanol−water solvent, of volume 770 Å^3 each, that add up to 25% of the cell volume (Speck, A. L. PLATON, A Multipurpose Crystallographic Tool, Utrecht University, 1999). Thermal treatment, monitored by XRPD, indicates that the network is retained after desolvation (up to ≈100 °C) and that guest water molecules can be readily reintroduced in the material by exposure to water vapors.

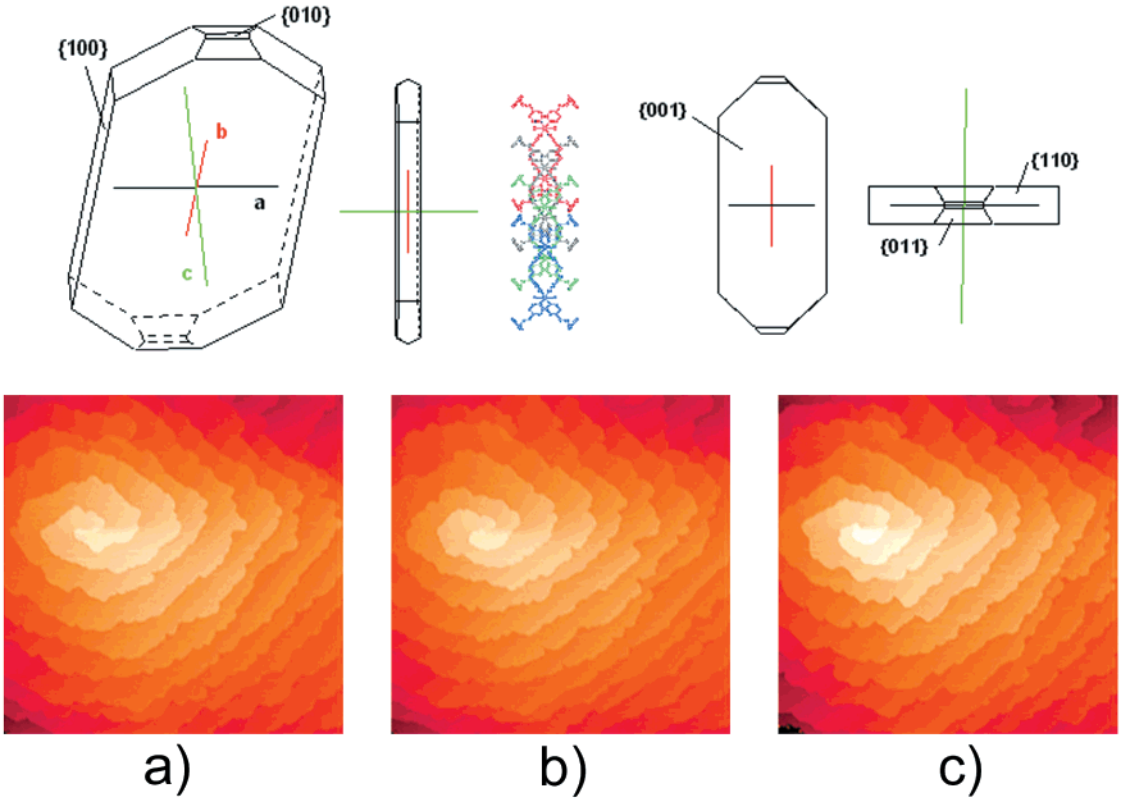

Figure 5. Top: correlation between crystal morphology and structure in compound **1**. Bottom: AFM monitoring of the crystal growth of **1** (scan size 2 × 2 μm^2) showing tangential accretion with monomolecular layers around a complex dislocation source.

Scheme 1

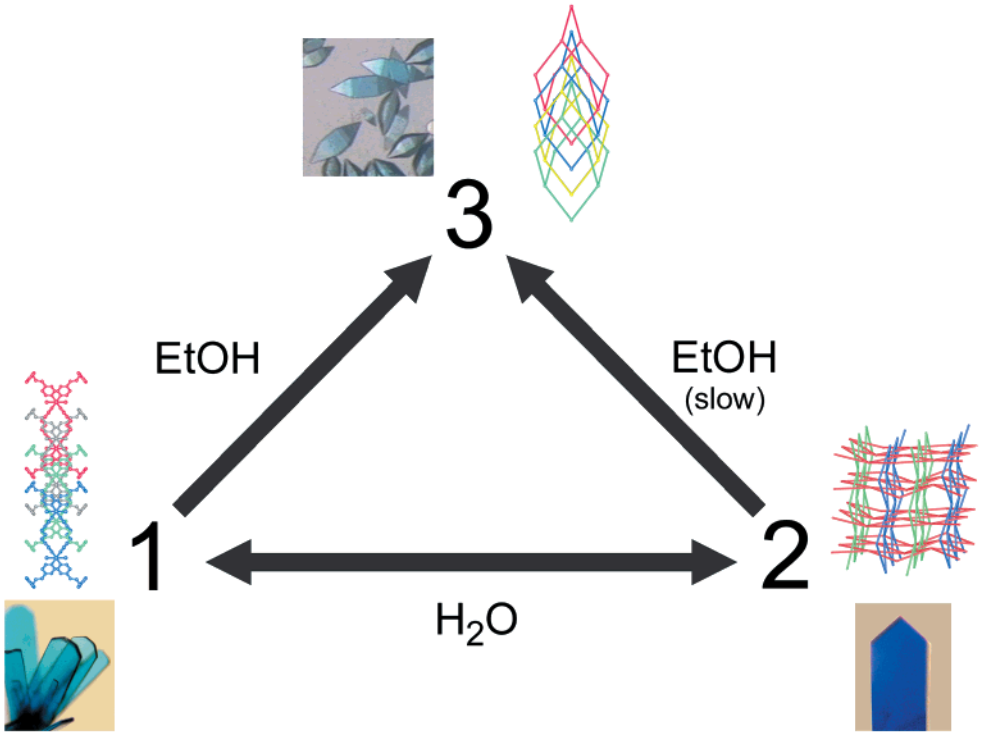

This has shown the following features: in compound **3** the highest growing rate is coincident with the tetragonal axis, along which the adamantanoid cages are interpenetrated. The most surprising result, however, is that in **1** the preferential growth direction of the crystals is along [0 1 0], which corresponds to the packing direction of the 1D polymers, coincident with the interdigitation of the chains, and not with the direction of extension of the chains along [1 0 0] (see Figure 5, top). Indeed, the periodic bond chain theory (PBC)[17] stresses the role, clearly recognized and tested,

(17) Hartman, P.; Perdok, W. G. *Acta Crystallogr.* **1955**, *8*, 49; **1955**, *8*, 521; **1955**, *8*, 525.

of intermolecular forces in determining the morphology of crystals[18] but, on this ground, we would expect the [1 0 0] growth direction to be the preferred one, owing to the more intense metal−ligand interactions.

Finally, preliminary studies with in situ AFM monitoring of the crystal growth of **1** reveals that this proceeds by tangential accretion of monomolecular layers (height of half of the **c** axis) corresponding to the (0 0 2) plane (Figure 5, bottom). Also on this scale the anisotropy of the interactions in the (0 0 1) plane shows growth rates ν[0 1 0] > ν[1 0 0], with profiles resembling those of the mature crystals.

We have pointed our attention to these kinds of studies about the crystallogenesis of the polymeric materials because they may be useful in achieving a better understanding of the driving factors operative in the self-assembly of the coordination networks. Besides the interesting features described here, this approach seems promising for general application to a variety of polymeric systems and supramolecular arrays.

Acknowledgment. We thank MURST for financing the project "Solid Supermolecules" 2000−2001.

Supporting Information Available: Crystallographic data for all the structures reported here (CIF). This material is available free of charge via the Internet at http://pubs.acs.org.

CM011235S

(18) Berkovitch-Yellin, Z. *J. Am. Chem. Soc.* **1985**, *107*, 8239.